Bands and interbands in $LaPd_3$ and $CePd_3$

C. Koenig and M. A. Khan
Groupe d'Etude des Materiaux Métalliques, Institut de Physique et Chimie des Materiaux de Strasbourg, Université Louis Pasteur, 4, rue Blaise Pascal, 67070 Strasbourg Cédex, France
(Received 21 March 1988)

A self-consistent calculation of the electronic structures of $LaPd_3$ and $CePd_3$ is presented. The method employed is that of the linear-muffin-tin orbitals with local-density approximation. The effects of spin-orbit coupling and those of $5p$ orbitals of La and Ce on the respective energy bands are studied. The energy bands and the density of states thus obtained are compared with available experimental data. The imaginary parts of the dielectric constant for the two compounds are calculated. The origins of different peaks in the optical spectra are traced back to interband transitions. The calculated optical properties of $CePd_3$ compare favorably with many existing data. For $LaPd_3$ some interesting optical peaks are obtained. This compound seems to be an ideal candidate to check the effects of $5p$ orbitals of La through optical measurements.

I. INTRODUCTION

The model calculation approach has been extensively used to explain the observed physical properties of rare-earth intermetallic compounds. These compounds have given rise to many interesting research initiatives due to their fluctuating valencies. First the electronic structures were explained through a "promotional model"[1] where the $4f$ electrons in Ce compounds were assumed to vary between 0 and 1. Later, this promotional model had to be discarded due to the fact that the spectroscopic measurements gave the f-electron count $\sim 0.8-1.2$.[2] Among these spectroscopic measurements, there have been the valence-band photoemission,[3-7] core-level x-ray photoemission (XPS),[8-11] and x-ray absorption (XAS).[2,9,10,12-16] The unoccupied states have also been studied by bremsstrahlung isochromat spectroscopy (BIS).[17,18] From the these experiments, it has been concluded that the many-body effects play an important role in the fluctuating valence compounds. In this context the extended Anderson's impurity model has been extensively used to explain different experimental observations.[17,19-21]

Besides studying individually the occupied or empty states, there have been a few attempts towards the study of the interband transitions in rare-earth intermetallic compounds and particularly in $CePd_3$.[22-25] Due to interband transitions, many structures are observed in the optical conductivity. Different authors have attributed these structures to different band-to-band transitions, since they did not have any *ab initio* band scheme of $CePd_3$ at their disposal. In spite of such a great deal of available experimental data, there have been only a few attempts to calculate *ab initio* energy bands of $LaPd_3$ and $CePd_3$. A self-consistent linearized-augmented-plane-wave (LAPW) calculation for $LaPd_3$ and $CePd_3$ has often been cited[26,27] but unfortunately, the details of this have never been published. Only the charge decomposition within each muffin-tin sphere has been tabulated.[27] Recently, another attempt to calculate the energy bands of $CePd_3$ by the LAPW method has been made.[28,29] A detailed study of the Fermi surface in $CePd_3$ is presented,[29] but these authors seem to be uninterested in the states away from the Fermi level. Their interest lies mainly in the heavy fermions.

In light of the above analysis of the present situation the necessity of the *ab initio* band schemes for $LaPd_3$ and $CePd_3$ becomes evident. It is also clear that any calculated band should not be focused only around the Fermi level but also at distant energies to understand the spectroscopic experiments such as the valence-band photoemission, XPS, XAS, and BIS. For a better insight into the optical measurements, it will be helpful to have a calculated dielectric constant where the band-to-band transitions are properly included. In the next section we present such a band scheme. The roles of $4f$ and $5p$ orbitals will be elaborated and then the importance of the spin-orbit interaction will be presented. In Sec. III the imaginary part of the dielectric constant and the optical conductivity obtained through the band scheme will be our main interest. Sections IV and V will be reserved, respectively, for discussion and conclusion.

II. ENERGY BANDS

Previous self-consistent calculations of the energy bands in $ScPd_3$ and YPd_3 (Refs. 30 and 31) by the method of linear-muffin-tin orbitals (LMTO) (Refs. 32-34) have shown that their physical properties are well accounted for within a band theory. The core charge distribution was obtained through the self-consistent Dirac atomic potential and then they were kept frozen for the energy-band calculations. The densities of states for these two compounds are very similar. They are constituted of two regions of high density: one below the Fermi level (E_F), corresponding to the $4d$ states of Pd, and one above E_F, corresponding to d states of Sc or Y. When going from $ScPd_3$ to YPd_3, one observes mainly an upward shift of E_F in the low-density region between the two d peaks, together with an increase of the charge transfer towards Pd and a decrease of the density of states at the Fermi level. This last observation is in quantitative agreement with specific-heat measurements.[35]

The situation becomes somewhat complicated in the case of $LaPd_3$ and $CePd_3$. These compounds are obviously more interesting since they are at the frontier of fluctuating valence systems. Two problems have then to be solved.

(1) The $4f$ states of La and Ce are in the vicinity of E_F and, at least for $CePd_3$, cannot be neglected. It is now well established that, as far as they are nearly empty and essentially step in through hybridization with other symmetries, these states can be treated together with the others in the local-density approximation (LDA).[26,27]

(2) The $5p$ core states of La or Ce are at about 0.8 Ry below the bottom of the conduction bands of the compounds. In the case of the isolated atoms, 0.20 and 0.27 $5p$ electrons of La and Ce, respectively, spread outside the Wigner-Seitz (WS) spheres. Thus, these states can no longer be considered as frozen core states in the crystal but have to be taken into account in the self-consistent band calculation, as a narrow band hybridized with the valence states.

These two points together with the fact that for narrow bands (especially $4f$ states), the third-order LMTO method is only valid in a relatively narrow energy interval around their center of gravity,[32] make the computational task delicate and more time consuming. In order to investigate the part played by the f levels and $5p$ core levels, we have performed a series of LMTO band-structure calculations for $LaPd_3$ and $CePd_3$ with the experimental lattice parameter 4.235 and 4.126 Å for $LaPd_3$ (Ref. 36) and $CePd_3$ (Ref. 37), respectively, with and without f states and also with and without $5p$ states in the core. These compounds crystallize in Cu_3Au crystal structure. The eigenvalues and eigenvectors were calculated on a grid of 165 k points in the irreducible wedge of the Brillouin zone (BZ). The scalar relativistic terms have been taken into account during the self-consistency and the spin-orbit coupling has been added as a perturbation on the converged potential.

The results concerning the number of electrons N_l for each l symmetry in the Wigner-Seitz spheres are given in Table I. Table II displays the departure from neutrality in each sphere, which is an indication for the strength of

TABLE I. (a) $LaPd_3$ and (b) $CePd_3$. Number of occupied states of each symmetry in the WS spheres of each type, per spin [(a) $R_{WS}=3.1286$ a.u.; (b) $R_{WS}=3.0480$ a.u.]. In the two-panel calculations, the lowest panel contains the bands arising from the $5p$ La states. In the last line, the numbers of states are given in the MT spheres.

(a) $LaPd_3$

l_{max} SO	Treatment of $5p$	La/spin N_s	N_p	N_d	N_f	3 Pd/spin N_s	N_p	N_d	N_f
2 No SO	Frozen	0.133	0.113	0.580		1.089	0.908	13.676	
2 No SO	Unfrozen								
	1st panel	0.0	2.828	0.0		0.042	0.066	0.063	
	2nd panel	0.137	0.114	0.660		1.082	0.910	13.595	
3 No SO	Frozen	0.127	0.105	0.538	0.089	1.084	0.872	13.566	0.118
3 No SO	Unfrozen								
	1st panel	0.0	2.807	0.0	0.0	0.042	0.066	0.064	0.020
	2nd panel	0.129	0.105	0.593	0.140	1.075	0.867	13.473	0.117
3 SO	Frozen	0.127	0.106	0.540	0.090	1.086	0.876	13.556	0.118
3 SO	Unfrozen								
	1st panel	0.0	2.804	0.0	0.0	0.043	0.067	0.065	0.020
	2nd panel	0.129	0.106	0.595	0.142	1.076	0.871	13.462	0.117
$R_{MT}=2.82$ a.u.[a]		0.07	0.09	0.475	0.185	0.81	0.51	13.125	

(b) $CePd_3$

l_{max} SO	Treatment of $5p$	Ce/spin N_s	N_p	N_d	N_F	3 Pd/spin N_s	N_p	N_d	N_f
3 No SO	Frozen	0.138	0.110	0.589	0.603	1.085	0.968	13.374	0.130
3 No SO	Unfrozen								
	1st panel	0.0	2.804	0.0	0.0	0.042	0.066	0.066	0.020
	2nd panel	0.139	0.110	0.623	0.650	1.077	0.961	13.309	0.130
3 SO	Frozen	0.137	0.110	0.587	0.642	1.083	0.956	13.354	0.130
3 SO	Unfrozen								
	1st panel	0.0	2.800	0.0	0.0	0.044	0.067	0.068	0.020
	2nd panel	0.138	0.110	0.620	0.691	1.074	0.949	13.287	0.130
$R_{MT}=2.765$ a.u.[a]		0.065	0.10	0.45	0.67	0.75	0.495	12.855	

[a]Reference 27.

the electron transfer towards the Pd atoms. The first remark is that there is but a little difference in the valence electron distribution from one calculation to another. In Figs. 1(a) [2(a)] and 1(b) [2(b)] we present the energy bands in $LaPd_3$ ($CePd_3$) when $5p$ orbitals are treated, respectively, as core states and as bands. These energy levels are given in the high-symmetry directions Γ-M-X-Γ-R-X. The effect of the spin-orbit coupling does not change the general layout of the energy bands, hence we do not give these dispersion curves here. The effects of the $5p$ orbitals on the density of states are presented in Figs. 3–6. Figures 3 and 5 present the total density of states (TDOS) and total number of states (TNOS) in $LaPd_3$ and $CePd_3$, respectively, when $5p$ orbitals are treated as core states. Figures 4 and 6 are the corresponding figures when $5p$ states are considered as bands. The effect of spin-orbit coupling in $CePd_3$ is represented in Fig. 7 where $5p$ orbitals are band states. In other words, Fig. 7 puts into evidence the spin-orbit (SO) effect on Fig. 6. The corresponding figure for $LaPd_3$ is not presented because the SO effect is similar to that in $CePd_3$.

III. INTERBAND TRANSITIONS

The optical response of a system is related to the complex dielectric function $\epsilon(q,\omega)$ with $q=0$ in the optical range (ω being the photon frequency);[38]

$$\epsilon(\omega)=\epsilon_1(\omega)+i\epsilon_2(\omega)\ . \tag{1}$$

The real and imaginary parts are expressed as

$$\epsilon_n(\omega)=\epsilon_n^f(\omega)+\epsilon_n^b(\omega),\quad n=1,2 \tag{2}$$

where the superscripts f and b indicate the free-electron

TABLE II. (a) $LaPd_3$. Band limits, total number N_{tot} of valence electrons in the WS of La and Pd atoms, departure from neutrality in each sphere (the electron transfer is from La to Pd). (b) The same as (a) for $CePd_3$.

(a) $LaPd_3$

l_{max} SO	Treatment of $5p$	E_{min} (Ry)	E_{max} (Ry)	E_F (Ry)	N_{tot} La	N_{tot} 3 Pd	ΔQ/atom La	ΔQ/atom Pd
2								
No SO	Frozen	−0.563		−0.116	1.653	31.347	1.347	−0.449
2	Unfrozen							
No SO	1st panel	−1.360	−1.331		5.657	0.343	0.343	−0.114
	2nd panel	−0.573		−0.136	1.824	31.176	1.176	−0.392
	Total						1.519	−0.506
3								
No SO	Frozen				1.718	31.282	1.282	−0.427
3	Unfrozen							
No SO	1st panel	−1.364	−1.341		5.616	0.384	0.384	−1.128
	2nd panel	−0.590		−0.167	1.935	31.065	1.065	−0.355
	Total						1.449	−0.483
3								
SO	Frozen	−0.581		−0.148	1.726	31.274	1.274	−0.425
3	Unfrozen							
SO	1st panel	−1.474	−1.467		5.608	0.391	0.391	−0.130
		−1.301	−1.281					
	2nd panel	−0.590		−0.167	1.946	31.053	1.053	−0.351
	Total						1.445	−0.481

(b) $CePd_3$

l_{max} SO	Treatment of $5p$	E_{min} (Ry)	E_{max} (Ry)	E_F (Ry)	N_{tot} Ce	N_{tot} 3 Pd	ΔQ/atom Ce	ΔQ/atom Pd
3								
No SO	Frozen	−0.597		−0.109	2.883	31.117	1.117	−0.372
3	1st panel	−1.404	−1.381		5.609	0.391	0.391	−0.130
No SO	2nd panel	−0.598		−0.121	3.044	30.955	0.955	−0.318
	Total						1.346	−0.448
3								
SO	Frozen	−0.597		−0.118	2.953	31.046	1.046	−0.349
3	1st panel	−1.525	−1.518		5.601	0.398	0.398	−0.132
SO		−1.336	−1.314					
	2nd panel	−0.598		−0.130	3.118	30.881	0.881	−0.294
	Total						1.280	−0.427

(Drude's term) and the band contributions, respectively. The band contribution is a function of the densities of states of occupied and empty bands and also of the transition probabilities from initial to final states. In practice it is sufficient to know either the real or the imaginary contribution and then to use the Kramers-Kronig transform to obtain the other. For a cubic material with volume Ω and in the limit of zero linewidth, the imaginary part $\epsilon_2(\omega)$ is written as

$$\epsilon_2(\omega)=\frac{8\pi^2e^2}{3m^2\omega^2\Omega}\sum_{n,n'}|P_{nn'}(\mathbf{k})|^2 f_n(\mathbf{k})[1-f_{n'}(\mathbf{k})] \times\delta(E_{n'}(\mathbf{k})-E_n(\mathbf{k})-\hbar\omega) \quad (3)$$

where $P_{nn'}(\mathbf{k})=\langle n'\mathbf{k}\,|\,P\,|\,n\mathbf{k}\rangle$ is the dipole matrix element between the initial $|\,n\mathbf{k}\rangle$ and final $|\,n'\mathbf{k}\rangle$ states with eigenvalues $E_n(\mathbf{k})$ and $E_{n'}(\mathbf{k})$, respectively. $f_n(\mathbf{k})$ is the Fermi-distribution function. At 0 K the above expression can be written as

$$\epsilon_2(\omega)=\frac{e^2}{3\pi m^2\omega^2}\sum_{n,n'}\int\frac{|P_{nn'}(\mathbf{k})|^2 dS}{|\nabla\omega_{nn'}(\mathbf{k})|} \quad (4)$$

where $S=\{\mathbf{k};E_{n'}(\mathbf{k})-E_n(\mathbf{k})=\omega_{nn'}(\mathbf{k})=\hbar\omega\}$. Now n and n' indicate the occupied and empty states, respectively. The integration is performed by the tetrahedron method.[39,40] The eigenfunctions $|\,nk\rangle$ obtained from the self-consistent band-structure calculation as described in the previous section are used to calculate the dipole-matrix elements $P_{nn'}(\mathbf{k})$. The details are given in a previous work.[41] Moreover, in a series of papers,[31,41–45] it has been established that $\epsilon_2(\omega)$ calculated with the help of the LMTO method is very satisfactory and reliable when

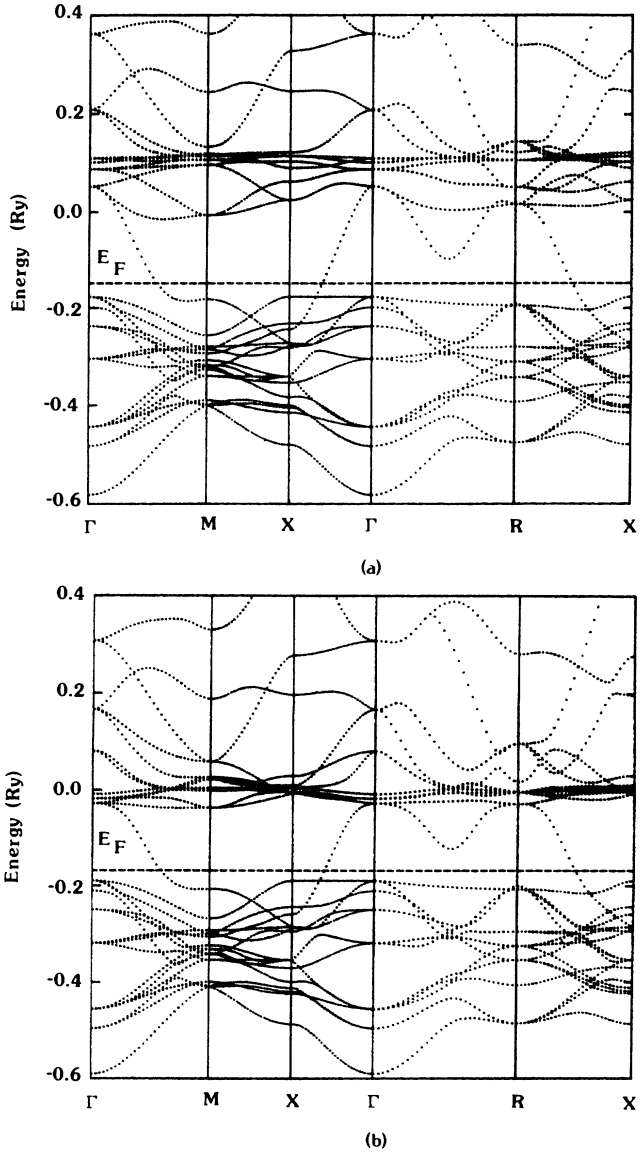

FIG. 1. Energy bands in $LaPd_3$ when $5p$ orbitals are localized (a) and when they are delocalized (b).

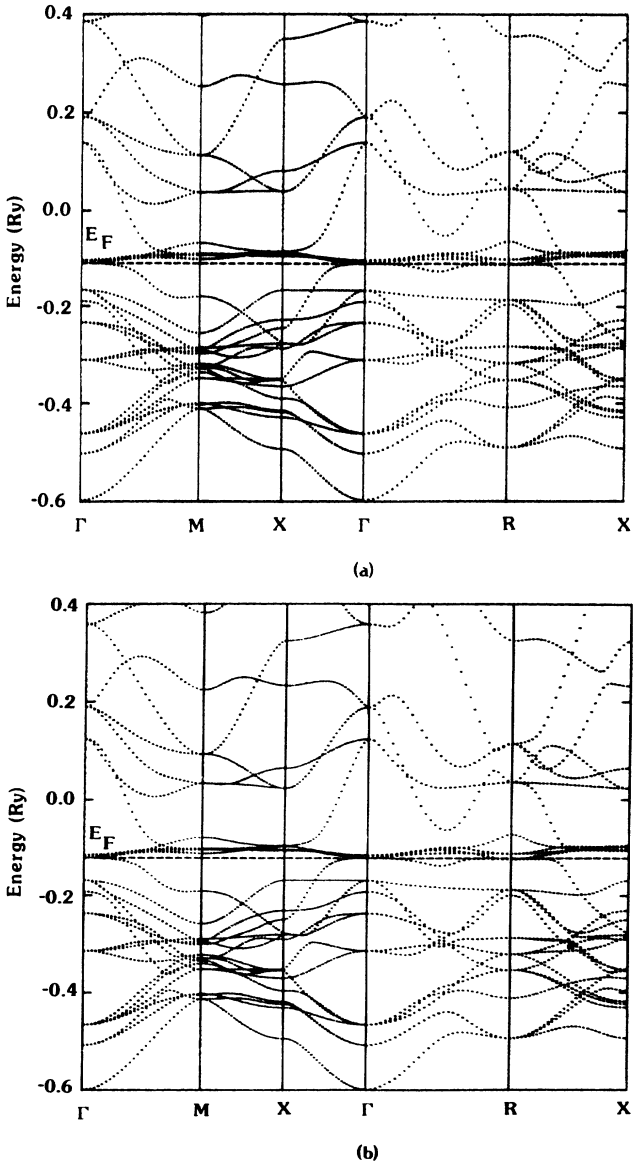

FIG. 2. Energy bands in $CePd_3$ when $5p$ orbitals are localized (a) and when they are delocalized (b).

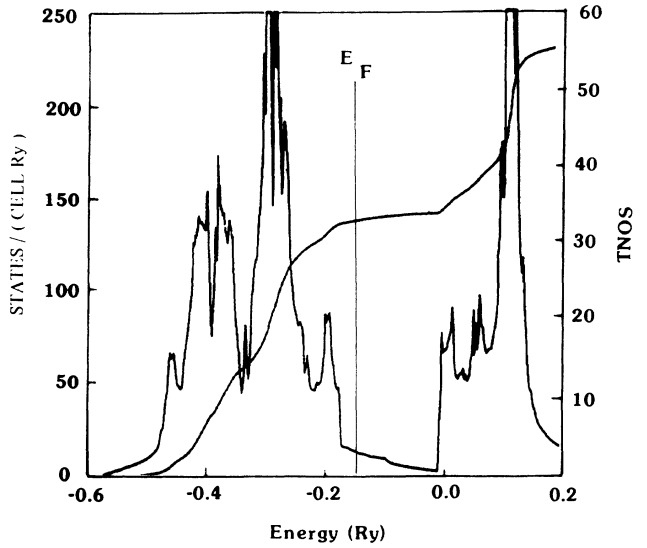

FIG. 3. Total density or states (TDOS) and total number of states (TNOS) in $LaPd_3$. $5p$ orbitals are localized.

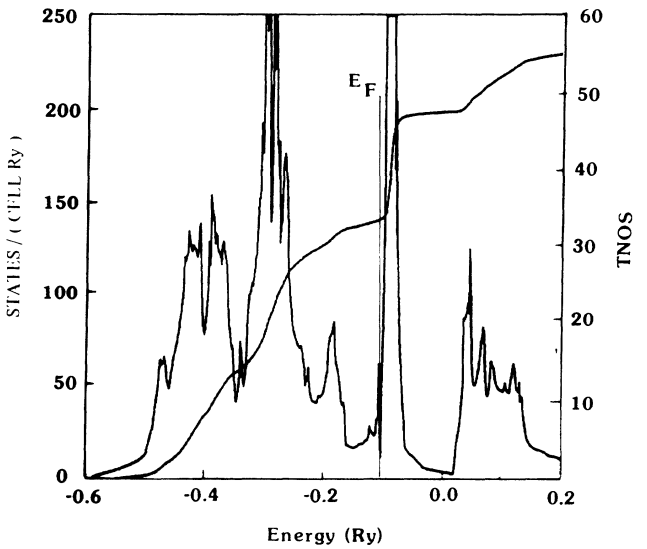

FIG. 5. TDOS and TNOS in $CePd_3$. $5p$ orbitals are localized.

compared to the experimental data in the low-energy range.

We have calculated $\epsilon_2(\omega)$ for $LaPd_3$ and $CePd_3$ for photon energy 0–0.4 Ry. We have used 165 **k** points in the irreducible part of the Brillouin zone. The calculations have been performed when $5p$ orbitals are core and band states. Starting from the lowest-energy level (Figs. 1 and 2), we have considered 30 levels for interband transitions. This way we are sure to include all the energy levels in the range of 0.4 Ry on both sides of the Fermi level. These calculated $\epsilon_2(\omega)$ are shown in Figs. 8–11. To facilitate the comparison of these curves with experimental data, they have been broadened through a Lorentzian with lifetime $\tau^{-1}=0.2$ eV. Also, we give the real part $\sigma_1(\omega)=\omega\epsilon_2(\omega)/4\pi$ of the optical conductivity in Figs. 12–15. We have not considered the spin-orbit effect on the optical properties and the reasons will be elaborated in the next section.

IV. DISCUSSION

A. Bands

1. Role of 4f states

We started the band calculation of $LaPd_3$ with s, p, and d electrons to obtain a self-consistent potential. This "poor man's calculation" gives satisfactory results for this compound: when recalculated in that potential the f states are correctly located, i.e., at about the same position above E_F as that obtained when they are included in

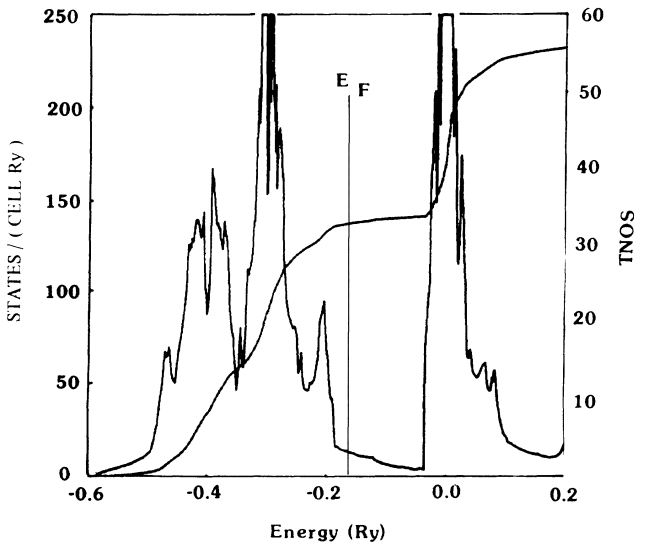

FIG. 4. TDOS and TNOS in $LaPd_3$. $5p$ orbitals are delocalized.

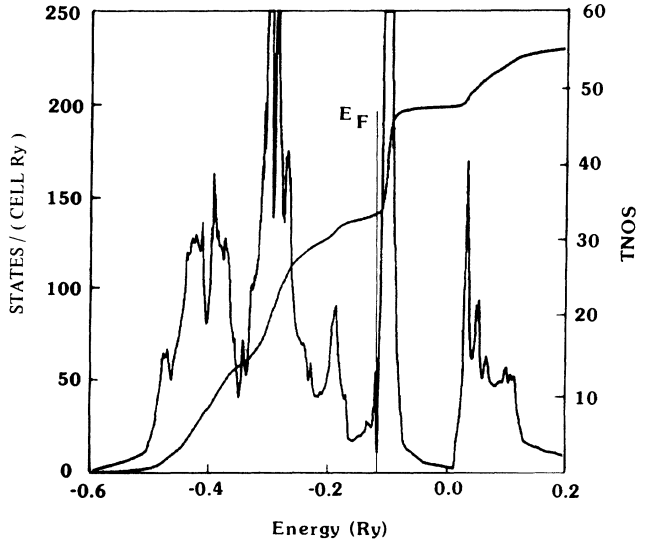

FIG. 6. TDOS and TNOS in $CePd_3$. $5p$ orbitals are delocalized.

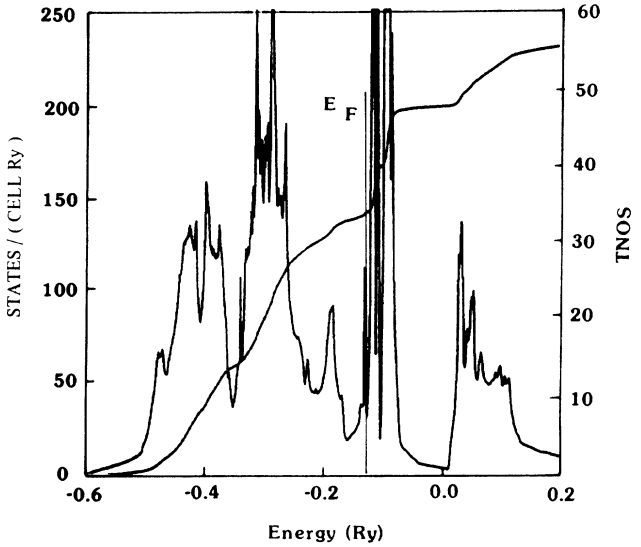

FIG. 7. TDOS and TNOS in $CePd_3$ with spin-orbit coupling. $5p$ orbitals are delocalized.

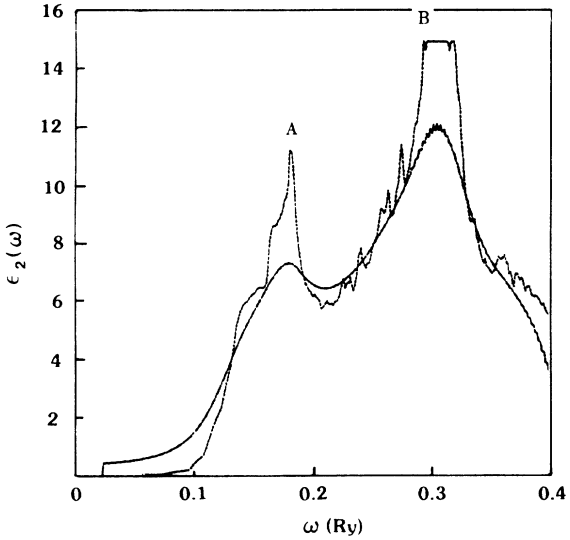

FIG. 9. $\epsilon_2(\omega)$ vs ω for $LaPd_3$ when $5p$ orbitals are delocalized.

the self-consistency. On the contrary the same procedure for $CePd_3$ yields an unphysical situation where the $4f$ states are located at about 0.7 Ry below E_F. Hence, the inclusion of the $4f$ states in the self-consistent process becomes a necessary condition to obtain the correct converged potential, whenever the $4f$ electrons are also in the occupied states and their hybridization with other symmetries plays an important role.

One has, then, to consider the exchange interactions and correlations for these f electrons. In the present calculation, the Hedin-Lundqvist approximation[46] including exchange and correlations is used for s, p, and d as well as for f occupied states. In his calculations Koelling[26,27] retains only the exchange potential, arguing that the inclusion of correlations unduly increases the weight of f states. Nevertheless, the number of occupied states per symmetry given by the present LMTO calculation is very similar to his LAPW results, with a slightly smaller f character (Table I). The numbers of electrons for each symmetry are given in muffin-tin (MT) spheres with radii $R_{MT}=2.820$ and 2.765 a.u. for $LaPd_3$ and $CePd_3$, respectively, by Koelling, whereas we give the corresponding numbers in Wigner-Seitz spheres of radii $R_{WS}=3.129$ and 3.048 a.u. for the respective compounds. Hence, the number of f electrons on La and Ce sites in Koelling's calculation will become even somewhat greater in Wigner-Seitz spheres. Considering the fact that the spherical approximation in each atomic sphere probably reinforces the weight of higher angular momentum,[28] one can conclude that the number of f occupied states in the Wigner-Seitz sphere of one Ce atom in $CePd_3$ is slightly larger than 1. These states are of itinerant character,

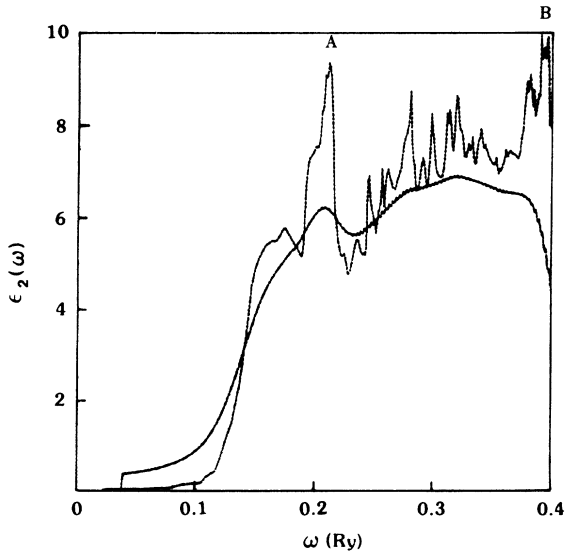

FIG. 8. $\epsilon_2(\omega)$ vs ω for $LaPd_3$ when $5p$ orbitals are localized.

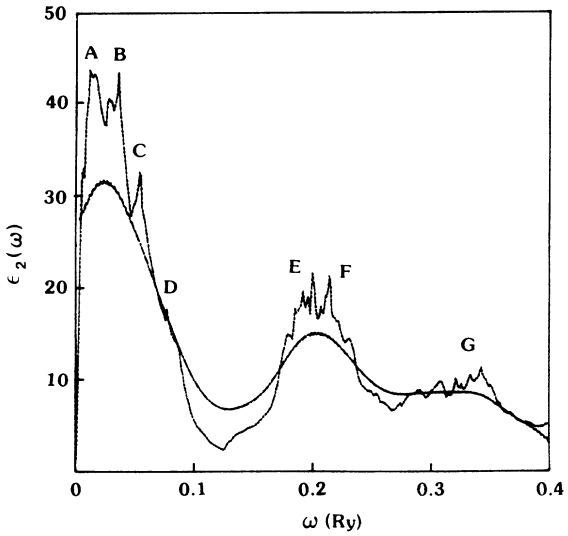

FIG. 10. $\epsilon_2(\omega)$ vs ω for $CePd_3$ when $5p$ orbitals are localized.

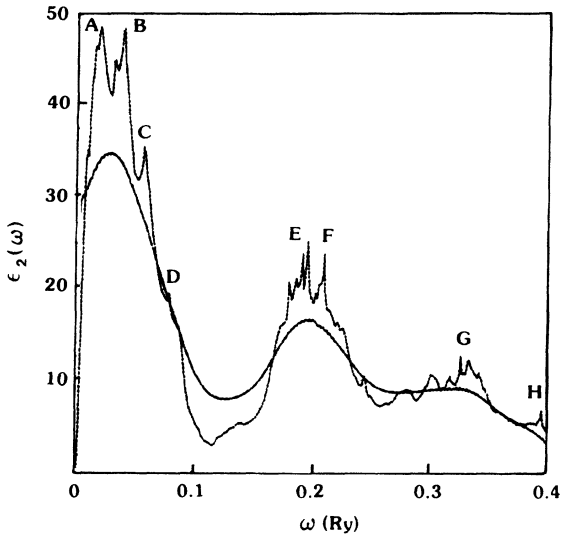

FIG. 11. $\epsilon_2(\omega)$ vs ω for $CePd_3$ when $5p$ orbitals are delocalized.

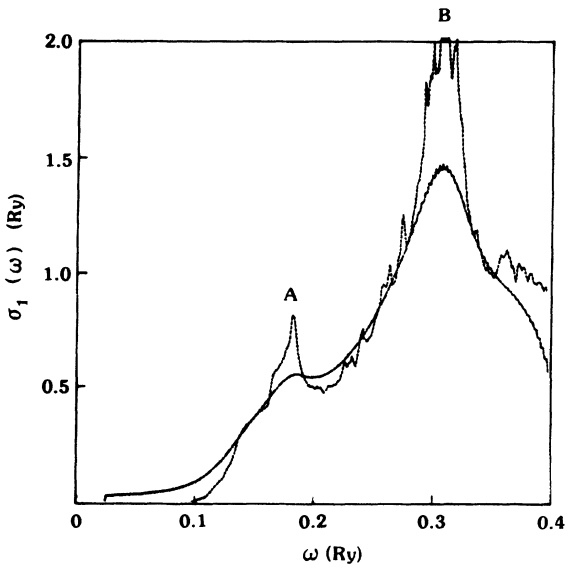

FIG. 13. The optical conductivity $\sigma_1(\omega)$ vs ω for $LaPd_3$ when $5p$ orbitals are delocalized.

essentially due to hybridization with other symmetries.

The s, p, and d partial densities of states for $LaPd_3$ and $CePd_3$ are very similar to those of $ScPd_3$ and YPd_3.[30] The Fermi level is in the pseudogap between the two regions of high d density. The f states form a very narrow peak which is superimposed on the partial La d density in $LaPd_3$, but lies in the pseudogap, just above E_F in $CePd_3$. When going through the series $ScPd_3$, YPd_3, $LaPd_3$, and $CePd_3$, one mainly observes a downward shift of this peak against a nearly rigid background of s, p, and d states.[47] The screening of the additional charge of the Ce nucleus compared to that of La is essentially provided by the available f states below E_F, leaving the Fermi level nearly unchanged.

2. *Role of 5p states*

From band-structure calculations of heavy compounds[48] it has been well established that a scalar relativistic model provides a good description of the conduction states. On the contrary, for inner shells, the spin-orbit coupling is non-negligible. Thus, the core states are better described by solving the full relativistic Dirac equations.

In the band-structure calculations presented here, the core states (i.e., [Kr], $4d^{10}$, $5s^2$ for La and Ce) are frozen in an atomic configuration corresponding to the free atoms. Their spatial charge distribution is obtained from a self-consistent relativistic Dirac program for isolated

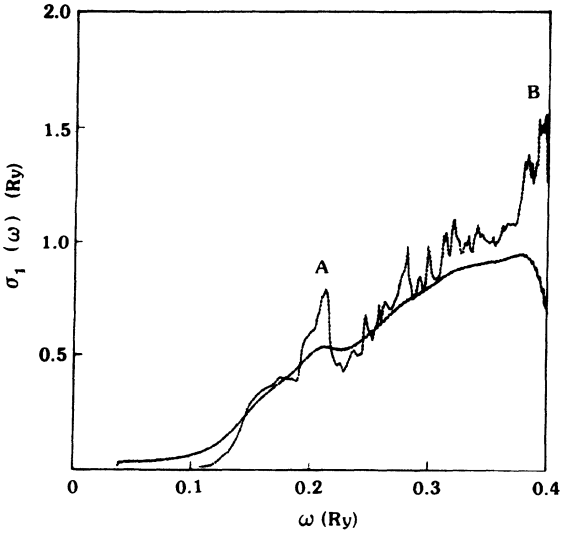

FIG. 12. The optical conductivity $\sigma_1(\omega)$ vs ω for $LaPd_3$ when $5p$ orbitals are localized.

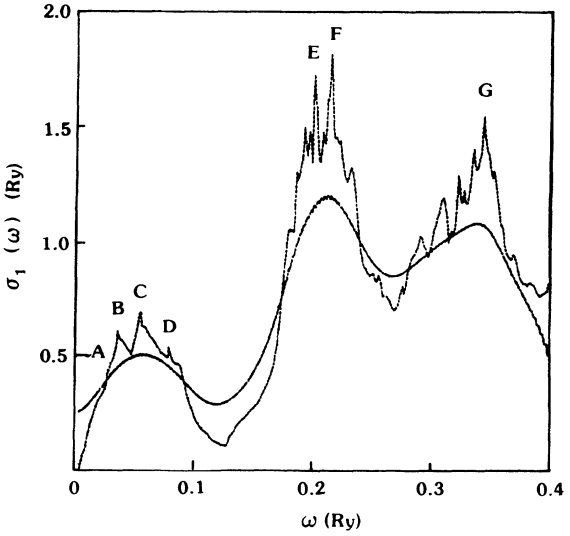

FIG. 14. the optical conductivity $\sigma_1(\omega)$ vs ω for $CePd_3$ when $5p$ orbitals are localized.

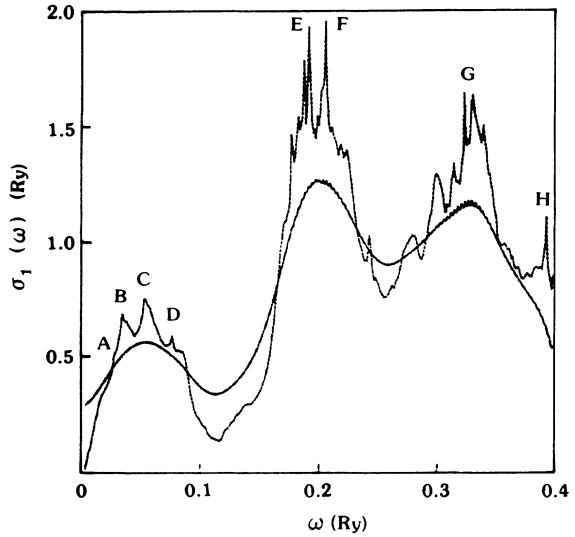

FIG. 15. The optical conductivity $\sigma_1(\omega)$ vs ω for $CePd_3$ when $5p$ orbitals are delocalized.

atoms or ions,[49] and is added to the conduction charge density to build the potential. In order to estimate the effect of using a frozen core approximation, different atomic configurations have been tested in the case of Ce: $4f^2 6s^2$ (free atom), $4f^0 5d^2 6s^2$, $4f^1 5d^1 6s^1 6p^1$, or even an ionic configuration: $4f^1 5d^1 6s^1$ which may simulate the effect of the transfer of one electron from Ce towards the Pd atoms in the compound. For example, in the $5d^2 6s^2$ configuration, the $4s$, $4p$, and $4d$ states are lowered about 7 eV compared to their positions in the free atom, and the $5s$ and $5p$ states are lowered, respectively, 3.2 and 2.5 eV; but the spatial distribution of the core states in the WS sphere is almost unaffected by their energy change.

In the compound $CePd_3$, the replacement of the core part of the free-atom charge distribution by the core part of one of the three other atomic configurations mentioned above induces no perceptible effect on the electronic structure of the conduction states (the change in the charge transfer for example is less than $\frac{1}{1000}e^-$). This justifies the frozen approximation used in these calculations for the inner shells of the atoms.

Now we discuss the effect of the spatial extension of the last of these core states ($5s$ and $5p$) outside the WS sphere of the La or Ce atom in the compound. As has already been mentioned earlier, we have explicitly studied the effect of $5p$ orbitals on the energy bands. First, these orbitals are considered frozen and their charge distribution is renormalized in the WS sphere. The calculations are performed in the energy panel which covers the valence-conduction-band region. Later, the orbitals are unfrozen and are treated as band states. Now, the calculations are performed in two energy panels, one from -1.60 to -1.2 Ry covering mainly the $5p$ states and the second covers the conduction bands. The lower band (first panel) arising from the delocalization of the $5p$ states contributes a non-negligible amount to the electron transfer towards the Pd atoms. Nearly 0.4 electrons leave the La (or Ce) sphere (Table II) to populate the Pd atoms. This transfer is more important than those of the $5p$ orbitals which lie outside the sphere in the isolated atomic potential. This induces a noticeable lowering of the total energy of the crystal.

Once the $5p$ states are removed from the La or Ce core, the remaining core still has 0.02 electrons outside the WS sphere, constituted mainly with the $5s$ states. But the $5s$ core level lies at -2.8 Ry, i.e., 1.4 Ry below the $5p$ states and too far below the muffin-tin zero potential ($V_{MTZ} \simeq -0.73$ Ry) to be reasonably treated by a LMTO band calculation. Thus, the $5s$ states are kept frozen and their charge distribution is renormalized in the WS sphere.

In $LaPd_3$, the delocalization of the $5p$ states induces a downward shift of the f peak, of about 0.1 Ry (Figs. 3 and 4). On the contrary, in $CePd_3$, this peak remains blocked just above E_F as in the frozen $5p$ calculation (Figs. 5 and 6). This can be explained by the fact that the attractive effect of the delocalization of the $5p$ states in this case induces an increase of the f occupied states which in its turn is compensated by an increase of the repulsive Coulomb interaction with other electrons and thus the f level remains almost unchanged. The effect of the $5p$ delocalization is more obvious on the empty states of $LaPd_3$. Thus, the experiments involving the unoccupied states such as XAS, BIS, and optical absorption should be analyzed more carefully to obtain an answer concerning the delocalization of $5p$ orbitals.

3. *Spin-orbit coupling*

The spin-orbit coupling has been added as a perturbation to the converged potential of $LaPd_3$, in the two-panel model ($5p$ as band states). For $CePd_3$, eight more iterations were performed with this coupling without a significant evolution of the results. The global effect is a slight lowering of the charge transfer, but essentially a decoupling of the $5p$ states into $\frac{1}{2}$ and $\frac{3}{2}$ and of $4f$ states into $\frac{5}{2}$ and $\frac{7}{2}$. The splitting of $5p$ states is about 2.5 eV and that of $4f$ is about 0.26 eV (Fig. 7).

The spin-orbit coupling is of little effect in $LaPd_3$, since the f states are still far above E_F. On the contrary, in $CePd_3$, it affects the nature and the density of the states at the Fermi level. Table III compares the calculated density of states at the Fermi level [i.e., $n(E_F)$] to the one that could be extracted from specific-heat measurements[35] (the phonon enhancement is supposed to be no larger than 0.6). The agreement for $ScPd_3$ and YPd_3 is good.[30] For $LaPd_3$ the calculated density is low as compared to those of $ScPd_3$ and YPd_3 but still ten times larger than the experimental value. The corresponding value obtained by Koelling[27] is 7.8, which is of the same order of magnitude as in the present work. From Figs. 3 and 5 it is evident that the number of states at E_F will not change appreciably when this level is shifted a few mRy on either side in energy. Thus the discrepancy between the theoretical values and the only experimental measurement is not clear. We think some further measurements are needed to clarify the situation.

For $CePd_3$, the density calculated with spin-orbit cou-

TABLE III. Calculated density of states at the Fermi level, specific-heat coefficient and "experimental" density of states: $n(E_F)_{expt}=3\gamma/\pi^2 k_B^2(1+\lambda)$, where λ is the phonon enhancement coefficient.

X Pd_3		$n(E_F)$ [(Ry cell)$^{-1}$]	γ^b (mJ/K^2 mol)	$n(E_F)_{expt}$ [(Ry cell)$^{-1}$] $\lambda=1$	$\lambda=0.6$
Sc (*spd*)	1 panel	38.8[a]	8.20	47.3	30.5
Y (*spd*)	1 panel	15.34[a]	3.48	20.0	12.5
La (*spdf*)	1 panel	12.55	0.28	1.6	1.0
	1 panel+SO	12.73			
	2 panels	13.48			
	2 panels+SO	13.73			
Ce (*spdf*)	1 panel	27.13	38.6	222	139
	1 panel+SO	48.6			
	2 panels	23.9			
	2 panels+SO	42.6			

[a]Reference 30.
[b]Reference 35.

pling is twice the one without coupling, but seems rather far below its experimental value, which is about 200 states/Ry cell. However, it must be noted that E_F is just at the verge of the high f peak and that the density rises above 200 at less than 0.01 Ry above E_F. Considering the accuracy of the LMTO method, our calculation shows that the large experimental increase of the specific-heat coefficient when going from $LaPd_3$ to $CePd_3$ could be accounted for by a standard band scheme, without appealing to heavy-fermion effects.

4. *Spectroscopy and bands*

The spectroscopic measurements of these compounds are abundant and varied. The valence-band photoemission spectra of $LaPd_3$ and $CePd_3$ (Refs. 3 and 6) show three high-density regions which are mainly due to d partial DOS of Pd. The experimental observations of Peterman *et al.*[6] have been reproduced in Fig. 16. The three high-density regions are marked with arrows. Figures 3–7 clearly show these high-density regions below E_F. Their relative positions and intensities are in agreement with the experimental spectra. The theoretical calculations indicate that above E_F, $LaPd_3$ in its fundamental state will have a high density of d and f symmetries of La overlapping each other. The influence of the delocalization of the $5p$ orbitals is that the f peak is shifted towards the lower energy by an amount of ~ 1.5 eV (Fig. 5) as compared to the situation where the $5p$ orbitals were frozen (Fig. 3). Thus a high-density peak at about 2.5 eV above E_F will have a mixed character of d and f of La according to the present band scheme. In Fig. 17 are shown the experimental situations of the empty states of $LaPd_3$ and $CePd_3$ as observed through BIS by Hillebrecht *et al.*[50] In this work the peaks marked with arrows have been attributed to purely d states. The BIS measurements give another more important peak at ~ 6 eV above E_F which does not find its existence in the one-electron band scheme.

The unoccupied states of $CePd_3$ do not change appreciably from frozen to unfrozen $5p$ orbitals. In both situations one obtains an intense Ce f state just above E_F and then at about 2.5 eV from E_F there is another peak of Ce d origin. All the experimental measurements do indicate the presence of these two high-density regions, but at the same time they also indicate another intense peak at ~ 5 eV above E_F (Refs. 50–52) which is absent in the present band scheme. To trace the origin of this high-energy peak, the so-called $4f^2$ state, a great deal of work has been done in the approximation of the Anderson's impurity model.[19–21] In these model calculations one is in the domain of many-body effects[20] which is beyond the one-

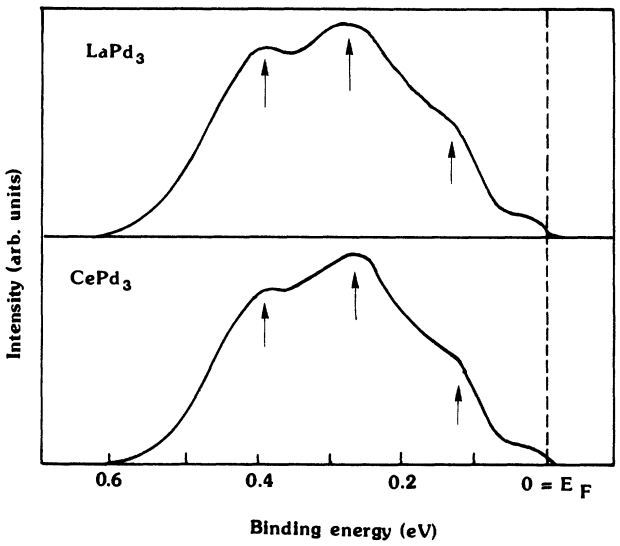

FIG. 16. Photoemission spectra of $LaPd_3$ and $CePd_3$ (Ref. 6).

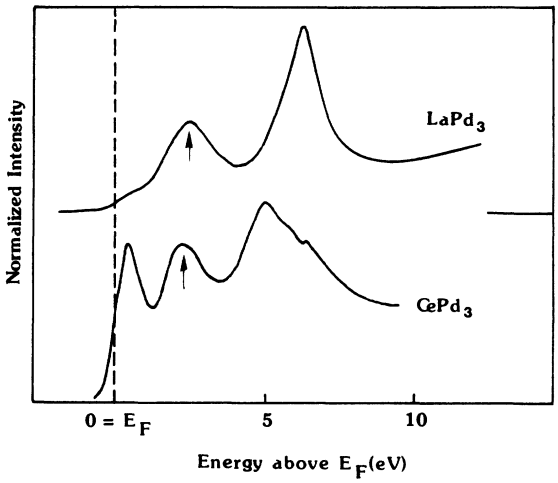

FIG. 17. BIS spectra of $LaPd_3$ and $CePd_3$ (Ref. 50).

electron band calculations. Recently, it has been argued[52] that the variation of the $4f^2$ splitting when compared with the free Ce^{2+} ion is due to some change in the nuclear charge ΔZ due to the delocalization of the core levels ($\Delta Z > 0$) or some screening effect of the valence electrons ($\Delta Z < 0$). According to the present study the delocalization of $5p$ orbitals does not bring any appreciable change in the DOS of $CePd_3$. As for the screening effect of the valence electrons on $4f^2$ orbitals, one will have to resort to the problem of a substitutional impurity in a matrix.[53–57] Of course this will be out of the context of the present work.

B. Interbands

1. $LaPd_3$

The optical properties of $LaPd_3$ and $CePd_3$ involving the interband transitions are presented in Figs. 8–15. Figures 8 and 9 show the $\epsilon_2(\omega)$ for $LaPd_3$ when $5p$ orbitals are localized and delocalized, respectively. Figures 12 and 13 show $\sigma_1(\omega)=\omega\epsilon_2(\omega)/4\pi$ for Figs. 8 and 9, respectively. These figures and also the corresponding figures (10, 11, 14, and 15) for $CePd_3$ have been Lorentzian broadened to take into account roughly the relaxation time effects. From Figs. 8 and 12 we observe the main optical structures at 2.84 (A) and 5.23 eV (B). In between there are many small structures which will be smoothed in an observed spectrum. When the $5p$ orbitals are delocalized we notice a downward shift of these peaks to 2.42 and 4.08 eV, respectively (Figs. 9 and 13). The first peak A is due to transitions from the highest (17th) occupied flat level (Fig. 1) in the Γ-X (Δ) direction to the 18th and 19th levels above E_F. The 17th level is predominantly of (Pd) d nature whereas the empty states (18th and 19th) are strongly of Ce character, but they also have 30% (Pd) p symmetry. This A peak is due to (Pd) $d \rightarrow p$ transition. Peak B is also of (Pd) $d \rightarrow p$ nature where the initial states are at about 1.7 eV below E_F and mainly in the X-R (Z) direction. The effect of delocalization of the $5p$ orbitals is evident in the case of $LaPd_3$ from the present work. Unfortunately, to our knowledge, so far there has been no experimental measurement of the optical conductivity in this compound.

2. $CePd_3$

From the dielectric constant, Figs. 10 and 11, and also from the optical conductivity, Figs. 14 and 15, we do not see any appreciable change due to delocalization of $5p$ orbitals of Ce in the low photon energy range. In the high-energy range (i.e., $\hbar\omega > 2$ eV), we notice some downward shift from the frozen $5p$ (Figs. 10 and 14) to unfrozen (Figs. 11 and 15) situation. In Table IV, we given the peak positions as obtained from these figures and also the corresponding experimental values when available.

We notice that according to the band theory, it is possible to observe many structures. At 1.06 eV (D) the structure is a slight shoulder in the corresponding figures and it is not surprising that experimentally it is not observed. Hence we shall talk no more of this structure except to add that it originates from (Pd) $d \rightarrow p$ transitions between the 16th and 20th energy levels near the high-symmetry point R (Fig. 2). The other high-energy peaks E and F will be lumped together due to the broadening effect and thus one will obtain a single peak centered at an energy between these two peaks. This convoluted peak and peak G are observed experimentally in almost all measured data.[22–24] All the high-energy peaks are due to (Pd) $d \rightarrow p$ interband transitions.

In the low-energy range (i.e., $\hbar\omega < 1$ eV) the attribution of the origin of these peaks differs from one work to another. In Refs. 22 and 23, peak A has been attributed to (Ce) $f \rightarrow d$ and (Ce) $d \rightarrow f$ interband transitions, respectively, whereas in Ref. 24, it is considered as an intraband effect (Ce) $f \rightarrow f$. We find its origin in the interband

TABLE IV. The optical peak positions (in eV) in $CePd_3$.

Peak positions	A	B	C	D	E	F	G	H
$5p$ frozen	0.24	0.47	0.77	1.06	2.67	2.81	4.55	
$5p$ unfrozen	0.24	0.47	0.77	1.06	2.63	2.78	4.46	5.29
Experiments								
Ref. 22	0.25		0.73			2.6	4.2	
Ref. 23	0.25		0.7			2.7	4.5	
Ref. 24	0.27		0.8			2.3	4.1	
Ref. 25	0.235							

transitions between the 17th and 18th energy levels. These band-to-band transitions take place at **k** points in the high-symmetry directions $\Lambda(\Gamma\text{-}R)$ and $S(X\text{-}R)$. Both these levels have a very high percentage of f electrons. In the Λ direction the 17th level is composed of 3.6% and 81% (Ce) d and (Ce) f symmetries and the 18th level is of 95% (Ce) f. In the S direction these levels are respectively of 3% (Ce) d and 63% (Ce) f (17th level) and 95% (Ce) f (18th level). The rest of the orbitals are of Pd nature. From these symmetry decompositions peak A should be attributed to (Ce) $d \rightarrow f$ transitions as done previously by Allen *et al.*[23]

According to the band scheme, the structure B at 0.47 eV (Figs. 10, 11, 14, and 15) is due to the transitions between the 17th and 19th energy levels in the high-symmetry direction Λ ($\Gamma\text{-}R$). It is also of (Ce) $d \rightarrow f$ nature. Peaks A and B are entirely due to band-to-band transitions and their separation is due to the band splitting in the Λ direction. Unfortunately, structure B is not observed experimentally. Peak C (0.77 eV) is due to the transition from the 16th to 18th level near Γ and is of (Pd) $d \rightarrow p$ nature. This observation is in agreement with the proposition of Schoenes and Andres.[22] Allen *et al.*[23] suggest (Ce) $f \rightarrow d$ whereas Hillebrands *et al.*[24] go one step further to invoke the intersite transitions (Pd) $d \rightarrow$ (Ce) f. Hillebrands *et al.*[24] propose the same kind of intersite transitions to explain the existence of the most intense peak at 2.3 eV (E, F).

On the whole our results are in good agreement with the interpretations given by Schoenes and Andres[22] except that for the low-energy peak A. To interpret this peak due to intraband effect Hillebrands *et al.*[24] have taken into consideration the spin-orbit separation of f states in $\frac{5}{2}$ and $\frac{7}{2}$ levels which is indeed of the order of 0.27 eV. Presently, we found that the spin-orbit splitting of f states is 0.26 eV, but both these split peaks are in the empty band region (Fig. 7). Moreover, we find that peak A is present even when spin-orbit coupling is absent in the band scheme and hence entirely an interband effect. Since all the observed optical peaks are already present in the calculated spectra, we do not consider it necessary to do any further investigation in the presence of SO coupling.

V. CONCLUSION

The self-consistent band structures of $LaPd_3$ and $CePd_3$ put into evidence that on the one hand the effect of the delocalization of $5p$ orbitals is very important in $LaPd_3$ and on the other hand the f orbitals play a prominent role in the case of $CePd_3$. The overall spin-orbit effect is rather secondary, because most of the experimental data could be explained without taking into consideration the SO coupling.

Our calculated optical spectra are rich in structure and promising for future work. The measured optical data of $CePd_3$ have been clearly interpreted with the help of intrasite interband transitions. The ambiguity of interpretations of spectra in different experiments has been removed. The predictions forwarded for $LaPd_3$ await confirmation through experimental measurements.

ACKNOWLEDGMENTS

It is our pleasure to acknowledge discussions with Professor E. Daniel and Professor A. Meyer and correspondence with Professor Syassen. We also benefited from the expert spectroscopic experience of Dr. J. Ringeissen and Dr. E. Beaurepaire. We thank them all. The Institut de Physique et Chimie des Materiaux de Strasbourg is "Unité Mixte No. 380046 au Centre National de la Recherche Scientifique, Université Louis Pasteur, et Ecole Européenne des haute étude des industries chimiques de Strasbourg."

[1] A. Iandelli and A. Palenzona, in *Handbook on the Physics and Chemistry of Rare Earths,* edited by K. A. Gschneidner, Jr. and L. Eyring (North-Holland, Amsterdam, 1979), Vol. II, p. 1.

[2] J. C. Fuggle, F. U. Hillebrecht, Z. Zołniereck, R. Lässer, Ch. Freiburg, O. Gunnarsson, and K. Schönhammer, Phys. Rev. B **27**, 7330 (1983).

[3] J. W. Allen, S.-J. Oh, I. Lindau, J. M. Lawrence, L. J. Johnsson, and S. B. M. Hagström, Phys. Rev. Lett. **46**, 1100 (1981).

[4] Y. Baer, H. R. Ott, J. C. Fuggle, and L. E. De Long, Phys. Rev. B **24**, 5384 (1981).

[5] M. Croft, J. H. Weaver, D. J. Peterman, and A. Franciosi, Phys. Rev. Lett. **46**, 1104 (1981).

[6] D. J. Peterman, J. H. Weaver, and M. Croft, Phys. Rev. B **25**, 5530 (1982).

[7] W. Gudat, M. Ivan, P. Pinchaux, and F. Hullinger, in *Valence Instabilities,* edited by P. Wachter and H. Boppart (North-Holland, Amsterdam, 1982), p. 249.

[8] J. C. Fuggle, M. Campagna, Z. Zołniereck, R. Lässer, and A. Platau, Phys. Rev. Lett. **45**, 1597 (1980).

[9] G. Krill and J. P. Kappler, J. Phys. C **14**, L1515 (1981).

[10] G. Krill, J. P. Kappler, A. Meyer, L. Abadli, and M. F. Ravet, J. Phys. F **11**, 1713 (1981).

[11] R. D. Parks, S. Raaen, M. L. den Boer, Y.-S. Chang, and G. P. Williams, Phys. Rev. Lett. **52**, 2176 (1984).

[12] F. U. Hillebrecht and J. C. Fuggle, Phys. Rev. B **25**, 3550 (1982).

[13] H. Launois, M. Rawiso, E. Holland-Moritz, R. Pott, and D. Wohlleben, Phys. Rev. Lett. **44**, 1271 (1980).

[14] R. D. Parks, S. Raaen, M. L. den Boer, V. Murgai, and T. Mihalisin, Phys. Rev. B **28**, 3556 (1983).

[15] B. Lengeler, M. Materlik, and J. E. Müller, Phys. Rev. B **28**, 2276 (1983).

[16] M. Croft, R. Neifeld, C. U. Serge, S. Raaen, and R. D. Parks, Phys. Rev. B **30**, 4164 (1984).

[17] F. U. Hillebrecht, J. C. Fuggle, G. A. Sawatzky, M. Campagna, O. Gunnarsson, and K. Schönhammer, Phys. Rev. B **30**, 1777 (1984).

[18] C. Laubschat, G. Kaindl, E. V. Sampathkumaran, and W. D. Schneider, Solid State Commun. **49**, 339 (1984).

[19] O. Gunnarsson and K. Schönhammer, Phys. Rev. Lett. **50**, 604 (1983).

[20] O. Gunnarsson and K. Schönhammer, Phys. Rev. B **28**, 4315

(1983).
[21]O. Gunnarsson, K. Schönhammer, J. C. Fuggle, F. C. Hillebrecht, J.-M. Esteva, R. C. Karnatak, and B. Hillebrands, Phys. Rev. B **28**, 7330 (1983).
[22]J. Schoenes and K. Andres, Solid State Commun. **42**, 359 (1982).
[23]J. W. Allen, R. J. Nemanich, and S.-J. Oh, J. Appl. Phys. **53**, 2145 (1982).
[24]B. Hillebrands, G. Güntherodt, R. Pott, W. König, and A. Breitschwert, Solid State Commun. **43**, 891 (1982).
[25]B. C. Webb, J. A. Sievers, and T. Mihalisin, Phys. Rev. Lett. **57**, 1951 (1986).
[26]D. D. Koelling, Solid State Commun. **43**, 247 (1982).
[27]D. D. Koelling, in The Electronic Structure of Complex Systems, NATO Advanced Study Institute, Ghent, Belgium, 1982 (unpublished).
[28]A. Yanasae, J. Magn. Magn. Mater. **70**, 73 (1987).
[29]A. Hasegawa and A. Yanasae, J. Phys. Soc. Jpn. **56**, 3990 (1987).
[30]C. Koenig, Z. Phys. B **50**, 33 (1983).
[31]M. Alouani, C. Koenig, and M. A. Khan, Solid State Commun. **65**, 327 (1988).
[32]O. K. Andersen, Phys. Rev. B **12**, 3060 (1975).
[33]O. K. Andersen, in *The Electronic Stucture of Complex Systems,* edited by P. Phariseau and W. M. Temmerman (Plenum, New York, 1984).
[34]H. L. Skriver, *The LMTO Method* (Springer, Berlin, 1984).
[35]M. J. Besnus, J. P. Kappler, and A. Meyer, J. Phys. F **13**, 597 (1983).
[36]A. Meyer (private communication).
[37]J. P. Kappler, G. Krill, M. J. Besnus, M. F. Ravet, N. Hamdaoui, and A. Meyer, J. Appl. Phys. **53**, 2152 (1982).
[38]D. Pines, *Elementary Excitations in Solids* (Benjamin, New York, 1964), p. 211.
[39]O. Jepsen and O. K. Andersen, Solid State Commun. **9**, 1763 (1971).
[40]G. Lehman and M. Taut, Phys. Status Solidi B **54**, 469 (1972).
[41]C. Koenig and M. A. Khan, Phys. Rev. B **27**, 6129 (1983).
[42]M. A. Khan, C. Koenig, and R. Riedinger, J. Phys. F **13**, L159 (1983).
[43]M. Alouani and M. A. Khan, J. Phys. (Paris) **47**, 453 (1986).
[44]M. Alouani, J. M. Koch, and M. A. Khan, J. Phys. F **16**, 473 (1986).
[45]N. I. Kulikov, M. Alouani, M. A. Khan, and M. V. Magnitskaya, Phys. Rev. B **36**, 929 (1987).
[46]L. Hedin and B. I. Lundqvist, J. Phys. C **4**, 2064 (1971).
[47]C. Koenig and M. A. Khan (unpublished).
[48]D. D. Koelling and B. M. Harman, J. Phys. C **10**, 3107 (1977).
[49]J. P. Desclaux, Comput. Phys. Commun. **9**, 31 (1975).
[50]F. U. Hillebrecht, J. C. Fuggle, G. A. Sawatzky, and R. Zeller, Phys. Rev. Lett. **51**, 1187 (1983).
[51]Y. Baer, H. R. Ott, J. C. Fuggle, and L. E. De Long, Phys. Rev. B **24**, 5384 (1983).
[52]C. Laubschat, W. Grentz, and G. Kaindl, Phys. Rev. B **36**, 8233 (1987).
[53]C. Koenig and E. Daniel, J. Phys. (Paris) Lett. **42**, L193 (1983).
[54]C. Koenig, P. Léonard, and E. Daniel, J. Phys. (Paris) **42**, 1015 (1983).
[55]C. Koenig, N. Stefanou, and J. M. Koch, Phys. Rev. B **33**, 5307 (1986).
[56]J. M. Koch, N. Stefanou, and C. Koenig, Phys. Rev. B **33**, 5319 (1986).
[57]M. Alouani, J. M. Koch, and M. A. Khan, Solid State Commun. **60**, 657 (1986).